

Nanoparticles for cardiovascular imaging and therapeutic delivery, Part 2: Radiolabeled probes

Short running title: Nanoparticles for cardiovascular imaging

John C. Stendahl^{1,2}, Albert J. Sinusas^{1,2,3}

July 2015

Word count: 1515

1. Department of Internal Medicine, Section of Cardiovascular Medicine, Yale University School of Medicine
2. Yale Translational Research Imaging Center, Yale University School of Medicine
3. Department of Diagnostic Radiology, Yale University School of Medicine

John C. Stendahl, MD, PhD; Postdoctoral Fellow
P.O. Box 208017
New Haven, CT 06516
Tel: (203) 735-5005, Fax: (203) 737-1030
john.stendahl@yale.edu

Albert J. Sinusas, MD
P.O. Box 208017
New Haven, CT 06516
Tel: (203) 735-5005, Fax: (203) 737-1030
albert.sinusas@yale.edu

JCS is supported by NIH T32 training grant number HL098069

Abstract

Nanoparticulate imaging agents and therapeutics have proven to be valuable tools in preclinical cardiovascular disease research. Due to their distinct properties and significant functional versatility, nanoparticulate imaging agents afford certain capabilities that are typically not provided by traditional small molecule agents. This review is the second in a two-part series covering nanoparticulate imaging agents and theranostics. It highlights current examples of radiolabeled nanoparticulate probes in preclinical cardiovascular research and demonstrates their utility in applications such as blood pool imaging and molecular imaging of ischemia, angiogenesis, atherosclerosis, and inflammation. These agents provide valuable insight into the molecular and cellular mechanisms of cardiovascular disease, and illustrate both the limitations and significant potential of nanoparticles in diagnostic and therapeutic applications. Further technological development to improve performance, address safety concerns, and fulfil regulatory obligations is required for clinical translation of these emergent technologies.

Key words: nanoparticles; cardiovascular disease; PET; SPECT; molecular imaging

Introduction

Nanoparticles have garnered significant interest as agents for cardiovascular imaging and therapeutic delivery. Nanoparticulate imaging agents typically demonstrate different pharmacokinetic and biodistribution behavior than small molecules and provide flexible platforms for integration of multiple functional entities, including targeting ligands, therapeutics, and/or multiple types of contrast materials. Importantly, nanoparticulate imaging agents are also capable of amplifying signals by delivering large volumes of contrast materials in concentrated packages. Despite these intriguing attributes, nanoparticulate imaging agents have thus far attained only limited clinical use and require additional development to overcome various functional limitations and safety concerns.

This review is the second in a two-part *JNM* series covering nanoparticulate imaging agents and theranostics. It describes current examples of radiolabeled nanoparticulate probes for positron emission tomography (PET) and single-photon emission computed tomography (SPECT), and highlights their utility in preclinical applications such as blood pool imaging and molecular imaging of ischemia, angiogenesis, atherosclerosis, and inflammation (Table 1). These agents provide valuable insight into the molecular and cellular mechanisms of cardiovascular disease, and illustrate both the limitations and significant potential of nanoparticles in diagnostic and therapeutic applications. Nanoparticle-based cardiovascular imaging via other modalities such as computed tomography (CT) and magnetic resonance (MR) has previously been reviewed in more detail elsewhere (1-4).

Ischemia

Radiolabeled nanoparticles have been utilized to detect and characterize ischemic and infarcted tissue, and to deliver relevant therapeutics. Although perfusion is reduced under conditions of ischemia and infarction, the associated vascular injury results in higher permeability than healthy tissue and allows for passive nanoparticle targeting via the enhanced permeability and retention (EPR) effect. Lukyanov et al. demonstrated this passively targeted delivery strategy by showing increased uptake of ^{111}In -labeled polymeric micelles in infarcted rabbit myocardium (5). In a separate study, $^{99\text{m}}\text{Tc}$ labeling was used to monitor retention of chitosan nanoparticles delivered by direct injection into ischemic myocardium (6). Similar, unlabeled chitosan particles containing vascular endothelial growth factor (VEGF) were shown to increase perfusion to the ischemic tissue one week after administration. Passively targeted delivery of therapeutics via nanoparticles has also been demonstrated in the ischemic brain, where ^{18}F -labeled liposomes containing hemoglobin were shown to preferentially deposit in the ischemic zone of a middle cerebral artery thrombosis model, despite very low perfusion levels (7).

Angiogenesis

Radiolabeled nanoparticles have also been utilized for targeted molecular detection and characterization of new microvessels formed by angiogenesis. Potential clinical applications of angiogenesis imaging within the cardiovascular system include characterization of ischemia-induced angiogenesis and detection of intraplaque angiogenesis that predisposes to plaque rupture. The most established molecular target for angiogenesis is the $\alpha_v\beta_3$ integrin, a heterodimeric transmembrane protein which is expressed on many cell types, but differentially upregulated on proliferating endothelial cells (8). Nanoparticles targeted towards $\alpha_v\beta_3$ integrins are well-suited for angiogenesis imaging because they can limit signals from non-angiogenic $\alpha_v\beta_3$ binding through multivalent ligand presentation and size-based vascular compartment confinement. Almutairi et al. successfully utilized ^{76}Br -labeled multivalent dendrimers with $\alpha_v\beta_3$ -targeted peptides for PET-CT detection of angiogenesis in a murine hind limb ischemia model (9) (Fig. 1). The power of presenting multiple $\alpha_v\beta_3$ binding epitopes on a single dendrimer surface is demonstrated by the fact that the multivalent dendrimers exhibited a 50-fold enhancement in $\alpha_v\beta_3$ binding affinity compared with monovalent free peptides. A variety of other types of nanoparticle platforms have been utilized for $\alpha_v\beta_3$ -mediated nuclear angiogenesis imaging, including gold particles (10), perfluorocarbon emulsions (11), carbon nanotubes (12), and lanthanide upconversion nanophosphors (13). Another potential molecular target for angiogenesis imaging is natriuretic peptide receptor-C (NPR-C), which was targeted with a novel comb-like polymeric nanoparticle functionalized with C-type atrial natriuretic factor (CANF) fragments and labelled with ^{64}Cu for PET imaging (14). This NPR-C-targeted nanoparticle probe was used to noninvasively detect angiogenesis in an established murine model of hind limb ischemia.

Blood pool imaging

Nanoparticles are also potentially useful as blood pool imaging agents because they can be designed for extended circulation with minimal extravasation into the surrounding tissue. Examples of nanoparticulate blood pool agents in nuclear imaging include multimodal dendrimers for SPECT-CT (15), multimodal cross-linked dextran iron oxide agents for PET-CT/MR (16), and core-shell star copolymers for PET (17). The long circulation times of these particles are primarily attributable to their intermediate sizes and surface functionalization with PEG moieties. These and other nanoparticulate agents may be useful for detection and characterization of ischemic heart and peripheral vascular diseases, including those related to microvascular dysfunction.

Given their capacity for extended circulation times, nanoparticulate blood pool agents are also potentially useful for defining vascular and cardiac structures. For example, nanoparticulate CT blood pool agents could be used with cine CT imaging for evaluation of the endocardial and epicardial surfaces. The use of this technique in combination with myocardial radiotracers in hybrid SPECT-CT or PET-CT imaging could allow for absolute radiotracer quantification with incorporation of partial volume corrections for regional differences in wall thickness. Long-circulating nanoparticulate agents are also particularly useful in small animal microSPECT-CT and microPET-CT blood pool imaging, where CT images may be acquired over periods of several minutes without the substantial clearance that occurs with conventional small molecule CT contrast agents (15).

Nanoparticulate SPECT and CT contrast agents which remain in the vascular compartment for extended periods could also be used to evaluate the myocardial microcirculation, which is the primary determinant of intramyocardial blood volume. Conventional small molecule contrast agents tend to overestimate intramyocardial blood volume due to significant first-pass myocardial extraction (18). Quantitative analysis of myocardial blood flow could also be accomplished via kinetic modeling of purely intravascular nanoparticle CT contrast agents imaged via high resolution dynamic cine CT (18).

Atherosclerosis

Radiolabeled nanoparticles are well-suited for detection and characterization of atherosclerotic lesions because their depth of tissue penetration typically does not exceed lesion thicknesses. Radiolabeled lipoprotein nanoparticles such as high-density lipoproteins (HDLs) and low-density lipoproteins (LDLs) have been used since the 1980s to monitor lipoprotein particle circulation and lipid uptake in atheromatous lesions (19-21). Endogenous HDL particles have dimensions on the order of 5-15 nm and are favorably suited for vascular imaging applications because of the ease at which they can be isolated and radiolabeled, and their intrinsic uptake in atherosclerotic lesions. Since initial studies nearly 30 years ago, numerous advances have been made, including the development of particles with synthetic or reconstituted lipoprotein shells that are designed for multimodal imaging and therapeutic delivery (22). Lipoprotein nanoparticles have also been utilized extensively in studies involving other, non-nuclear imaging modalities, such as MR; a review of this literature is available elsewhere (23).

Radiolabeled nanoparticles have also played significant roles in recent efforts to characterize intraplaque inflammation, which can induce thinning of fibrous caps on lesions and make them vulnerable to rupture. Nanoparticles targeted towards inflammatory cells have proven to be effective agents for detecting intraplaque inflammation and may provide ideal substrates for delivering

interventional payloads to stabilize plaques before they rupture and cause serious vascular events. Recent examples of nanoparticle-targeted intra-plaque inflammatory cell imaging include ^{64}Cu -labeled dendrimers targeted towards macrophages with LyP-1 peptides (PET-CT) (24), ^{64}Cu -labeled synthetic polymer particles targeted towards chemokine receptor-5 (CCR5) on monocytes (PET-CT) (25) (Fig. 2), and ^{89}Zr -labeled dextran nanoparticles passively-targeted towards intraplaque monocytes and macrophages (PET-MR) (26) (Fig. 3). In this last case, separate lipid nanoparticles containing siRNA to silence chemokine receptor-2 (CCR2), a receptor involved in recruitment of inflammatory monocytes (27), were also passively delivered to plaque monocytes and macrophages. Decreased uptake of ^{89}Zr -labeled dextran nanoparticles after targeted siRNA delivery demonstrated the potential of this approach for vulnerable plaque detection and preemptive stabilization.

Of related interest, van der Valk et al. recently published results of a first-in-human trial of liposome-mediated delivery of the anti-inflammatory drug prednisolone to atheromata (28). While *ex vivo* analysis demonstrated successful liposomal delivery to plaque macrophages, no decreases in vessel permeability were detected with dynamic contrast enhanced-MR imaging and no localized anti-inflammatory effects were detected with ^{18}F -fluorodeoxyglucose (FDG) PET-CT. Despite the lack of efficacy, this study importantly demonstrates the clinical feasibility of nanomedicinal delivery to atherosclerotic plaques and illustrates the potentially complementary roles of nanomedicine and advanced imaging in the clinical management of cardiovascular disease.

Additional cardiovascular applications of inflammatory cell imaging

Inflammatory cell imaging via radiolabeled nanoparticles has also been applied to other areas of diagnostic cardiovascular imaging research. Ueno et al. utilized PET-CT and passively targeted dextran-coated iron oxide (CLIO) nanoparticles labeled with ^{64}Cu to quantify myeloid cell infiltration in murine cardiac allografts and predict graft rejection and survival (29) (Fig. 4). The same laboratory also utilized PET-CT imaging with passively targeted ^{18}F -CLIO nanoparticles to quantify aortic aneurysm (AA) macrophages in a murine AA model (30). They were able to demonstrate in this pilot study that the magnitude of the macrophage-targeted PET-CT signal had predictive value for dimensional stability of aneurysms.

Conclusion

The diverse array of nanoparticulate imaging agents and theranostics described above illustrates the current utility of nanoparticles in cardiovascular imaging and therapy. These agents provide

valuable insight into the molecular and cellular mechanisms of cardiovascular disease, and illustrate both the limitations and significant potential of nanoparticles in diagnostic and therapeutic applications. Further technological development to improve performance, address safety concerns, and fulfil regulatory obligations is required for clinical translation of these emergent technologies.

Disclosures and acknowledgments

Drs. Sinusas and Stendahl have no conflicts of interest to disclose. Dr. Stendahl is supported by NIH T32 training grant number HL098069.

References

1. Strijkers GJ. Targeted Nanoparticles for Cardiovascular Molecular Imaging. *Curr Radiol Rep.* 2013;1:191-204.
2. Mulder WJM, Jaffer FA, Fayed ZA, Nahrendorf M. Imaging and Nanomedicine in Inflammatory Atherosclerosis. *Sci Transl Med.* 2014;6:1-11.
3. Chen HH, Josephson L, Sosnovik DE. Imaging of apoptosis in the heart with nanoparticle technology. *Wiley Interdiscip Rev Nanomed Nanobiotechnol.* 2011;3:86-99.
4. Chen W, Cormode DP, Fayad ZA, Mulder WJ. Nanoparticles as magnetic resonance imaging contrast agents for vascular and cardiac diseases. *Wiley Interdiscip Rev Nanomed Nanobiotechnol.* 2011;3:146-161.
5. Lukyanov AN, Hartner WC, Torchilin VP. Increased accumulation of PEG-PE micelles in the area of experimental myocardial infarction in rabbits. *J Control Release.* 2004;94:187-193.
6. Hwang H, Kwon J, Oh P-S, et al. Peptide-loaded Nanoparticles and Radionuclide Imaging for Individualized Treatment of Myocardial Ischemia. *Radiology.* 2014;273:160-167.
7. Urakami T, Kawaguchi AT, Akai S, et al. In vivo distribution of liposome-encapsulated hemoglobin determined by positron emission tomography. *Artif Organs.* 2009;33:164-168.
8. Brooks PC, Clark RAF, Chersesh DA. Requirement of Vascular Integrin $\alpha_v\beta_3$ for Angiogenesis. *Science.* 1994;264:569-571.
9. Almutairi A, Rossin R, Shokeen M, et al. Biodegradable dendritic positron-emitting nanoprobe for the noninvasive imaging of angiogenesis. *Proc Natl Acad Sci U S A.* 2009;106:685-690.
10. Morales-Avila E, Ferro-Flores G, Ocampo-Garcia BE, et al. Multimeric system of ^{99m}Tc -labeled gold nanoparticles conjugated to c[RGDfK(C)] for molecular imaging of tumor $\alpha(v)\beta(3)$ expression. *Bioconjug Chem.* 2011;22:913-922.
11. Lijowski M, Caruthers S, Hu G, et al. High-resolution SPECT-CT/MR molecular imaging of angiogenesis in the Vx2 model. *Invest Radiol.* 2009;44:15-22.
12. Liu Z, Cai W, He L, et al. In vivo biodistribution and highly efficient tumour targeting of carbon nanotubes in mice. *Nat Nanotechnol.* 2007;2:47-52.

13. Lee J, Lee TS, Ryu J, et al. RGD peptide-conjugated multimodal NaGdF₄:Yb³⁺/Er³⁺ nanophosphors for upconversion luminescence, MR, and PET imaging of tumor angiogenesis. *J Nucl Med.* 2013;54:96-103.
14. Liu Y, Pressly ED, Abendschein DR, et al. Targeting angiogenesis using a C-type atrial natriuretic factor-conjugated nanoprobe and PET. *J Nucl Med.* 2011;52:1956-1963.
15. Criscione JM, Dobrucki LW, Zhuang ZW, et al. Development and application of a multimodal contrast agent for SPECT/CT hybrid imaging. *Bioconjug Chem.* 2011;22:1784-1792.
16. Devaraj NK, Keliher EJ, Thurber GM, Nahrendorf M, Weissleder R. ¹⁸F Labeled Nanoparticles for *in Vivo* PET-CT Imaging. *Bioconjug Chem.* 2009;20:397-401.
17. Fukukawa K-I, Rossin R, Hagooly A, et al. Synthesis and Characterization of Core-Shell Star Copolymers for *In Vivo* PET Imaging Applications. *Biomacromolecules.* 2008;9:1329-1339.
18. Canty JM, Judd RM, Brody AS, Klocke FJ. First-Pass Entry of Nonionic Contrast Agent Into the Myocardial Extravascular Space. *Circulation.* 1991;84:2071-2078.
19. Sinzinger H, Bergmann H, Kaliman J, Angelberger P. Imaging of human atherosclerotic lesions using ¹²³I-low-density lipoprotein. *Eur J Nucl Med.* 1986;12:291-292.
20. Shaish A, Keren G, Chouraqui P, Levkovitz H. Imaging of Aortic Atherosclerotic Lesions by ¹²⁵I-LDL, ¹²⁵I-Oxidized-LDL, ¹²⁵I-HDL and ¹²⁵I-BSA. *Pathobiology.* 2001;2001:225-229.
21. Iuliano L, Signore A, Vallabajosula S, et al. Preparation and biodistribution of ^{99m}technetium labelled oxidized LDL in man. *Atherosclerosis.* 1996;126:131-141.
22. Jung C, Kaul MG, Bruns OT, et al. Intraperitoneal injection improves the uptake of nanoparticle-labeled high-density lipoprotein to atherosclerotic plaques compared with intravenous injection: a multimodal imaging study in ApoE knockout mice. *Circ Cardiovasc Imaging.* 2014;7:303-311.
23. Fay F, Sanchez-Gaytan BL, Cormode DP, et al. Nanocrystal Core Lipoprotein Biomimetics for Imaging of Lipoproteins and Associated Diseases. *Curr Cardiovasc Imaging Rep.* 2013;6:45-54.
24. Seo JW, Baek H, Mahakian LM, et al. ⁶⁴Cu-labeled LyP-1-dendrimer for PET-CT imaging of atherosclerotic plaque. *Bioconjug Chem.* 2014;25:231-239.
25. Luehmann HP, Pressly ED, Detering L, et al. PET/CT imaging of chemokine receptor CCR5 in vascular injury model using targeted nanoparticle. *J Nucl Med.* 2014;55:629-634.

- 26.** Majmudar MD, Yoo J, Keliher EJ, et al. Polymeric nanoparticle PET/MR imaging allows macrophage detection in atherosclerotic plaques. *Circ Res.* 2013;112:755-761.
- 27.** Leuschner F, Dutta P, Gorbato R, et al. Therapeutic siRNA silencing in inflammatory monocytes in mice. *Nat Biotechnol.* 2011;29:1005-1010.
- 28.** van der Valk FM, van Wijk DF, Lobatto ME, et al. Prednisolone-containing liposomes accumulate in human atherosclerotic macrophages upon intravenous administration. *Nanomedicine.* 2015;11:1039-1046.
- 29.** Ueno T, Dutta P, Keliher E, et al. Nanoparticle PET-CT detects rejection and immunomodulation in cardiac allografts. *Circ Cardiovasc Imaging.* 2013;6:568-573.
- 30.** Nahrendorf M, Keliher E, Marinelli B, et al. Detection of macrophages in aortic aneurysms by nanoparticle positron emission tomography-computed tomography. *Arterioscler Thromb Vasc Biol.* 2011;31:750-757.

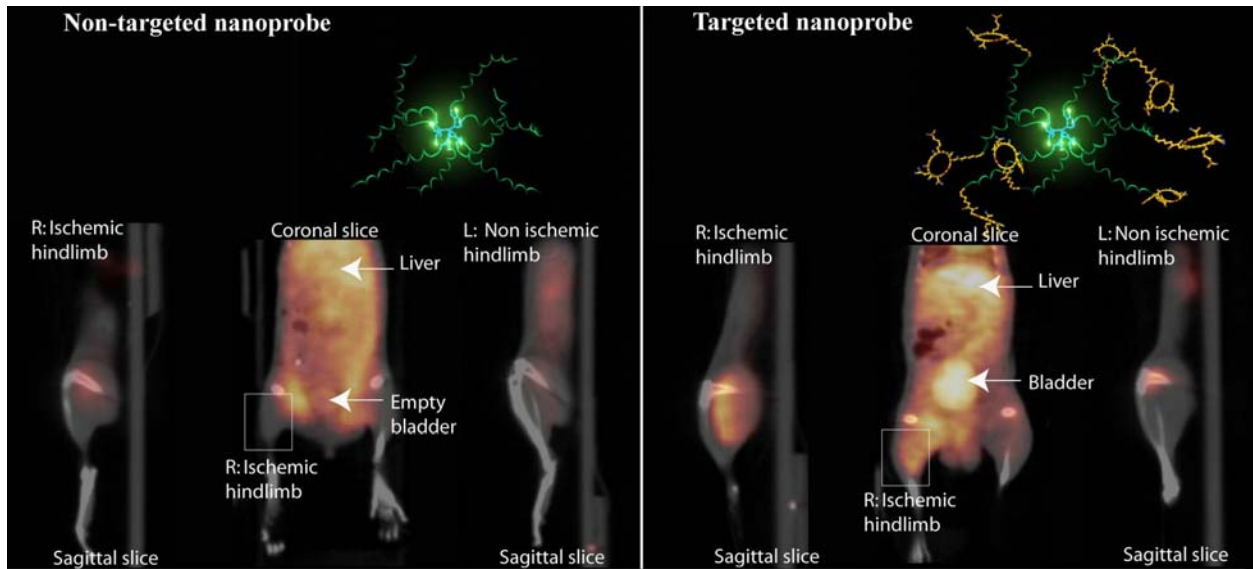


FIGURE 1. PET-CT images from reference 9 of angiogenesis in a murine hind limb ischemia model. Animals were injected with ^{125}I -labeled dendrimers 24 hours prior to imaging. There is significantly greater PET signal in ischemic limb muscle imaged with $\alpha_v\beta_3$ -targeted dendrimers (**B**) as compared to non-targeted dendrimers (**A**). Reprinted with permission of reference 9 (© 2009 by the authors and the National Academy of Sciences of the United States of America).

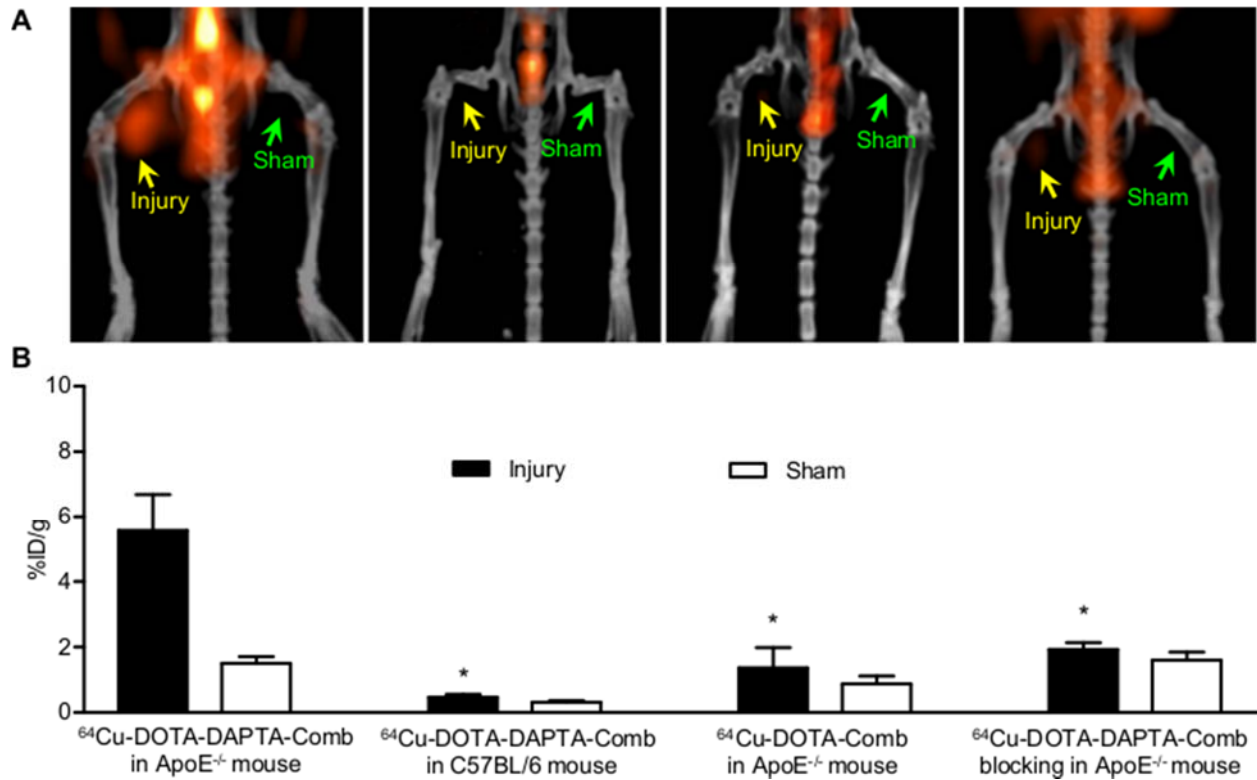


FIGURE 2. A. 24 hour maximum intensity PET-CT projection images from reference 25 showing uptake of ^{64}Cu -labelled comb-like polymer nanoparticles in a wire-injury-induced murine atherosclerosis model at two weeks post-injury. Nanoparticles displaying D-Ala₁-peptides (DAPTA) which bind chemokine receptor 5 (CCR5) in inflamed atheromas exhibited substantially greater uptake in atherosclerosis-susceptible ApoE^{-/-} mice than non-ApoE^{-/-}, non-DAPTA, and DAPTA-blocked controls. **B.** Quantification of nanoparticle uptake in corresponding images. Data are mean \pm SEM (* P < 0.001). Collectively, these images demonstrate the potential utility of CCR5-targeted nanoparticles in the imaging of atherosclerotic lesions. Reprinted with permission of reference 25 (© 2014 by the Society of Nuclear Medicine and Molecular Imaging, Inc.).

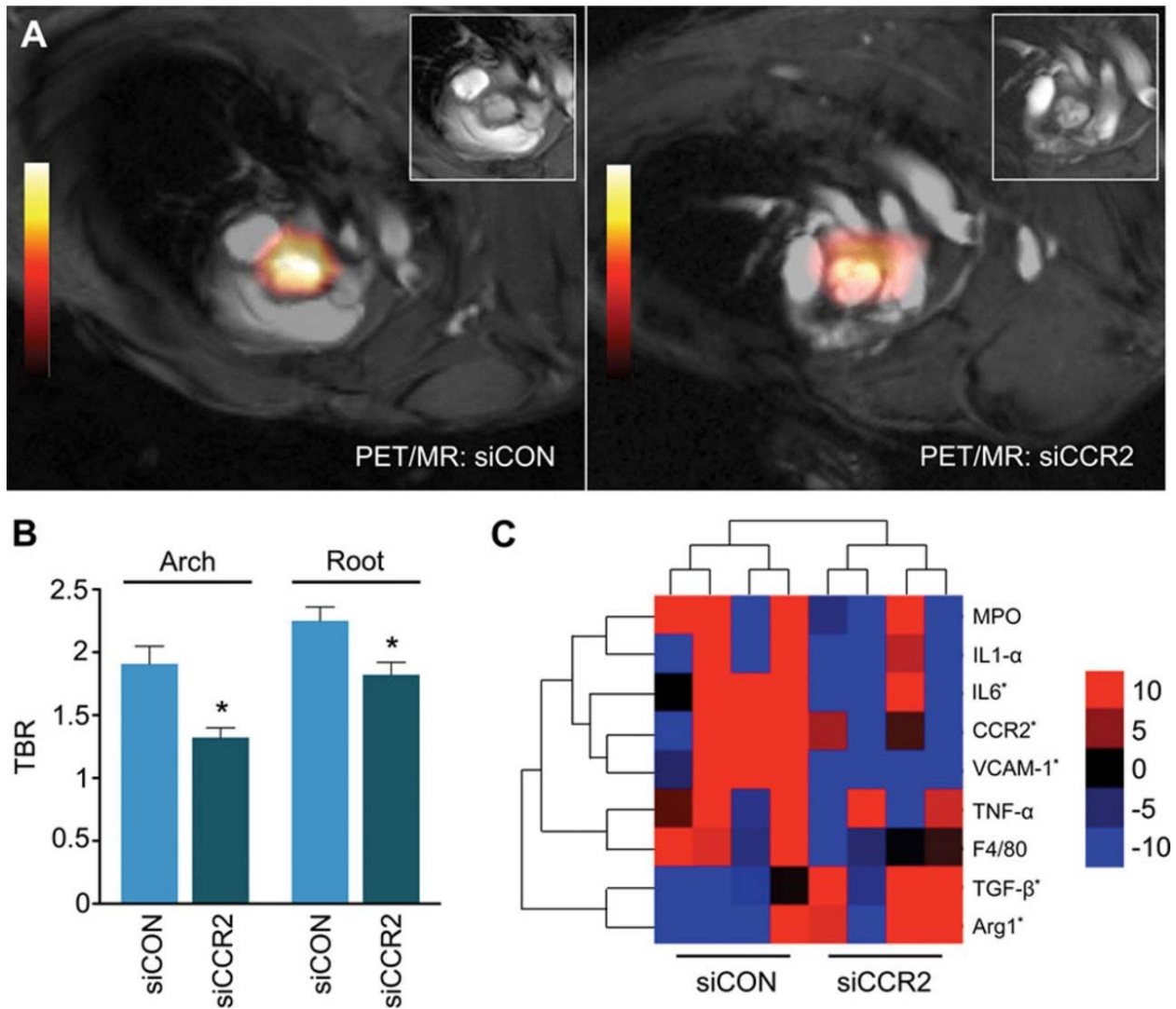


FIGURE 3. A. Representative PET-MR images from reference 26 showing uptake of ^{89}Zr -dextran nanoparticles passively targeted toward monocytes and macrophages in aortic plaques of apolipoprotein E-deficient mice. Prior to imaging, mice were treated with separate lipid nanoparticles containing either control siRNA (siCON) or siRNA to silence chemokine receptor-2 (siCCR2). **B.** Mean target-to-background ratios (TBR) from PET images showing siCCR2-nanoparticle-related suppression of PET signals due to attenuated monocyte recruitment ($n = 5$ per group; error bars represent SEM, $*P < 0.05$). **C.** Heat map of gene expression in aortic roots for siCON and siCCR2 subjects ($n = 4$ per group), where red indicates increased expression and blue indicates decreased expression (Arg1, arginase 1; IL, interleukin; MPO, myeloperoxidase; TGF, transforming growth factor; TNF, tumor necrosis factor; VCAM, vascular cell adhesion molecule; F4/80 is a murine macrophage marker). Reprinted from reference 26.

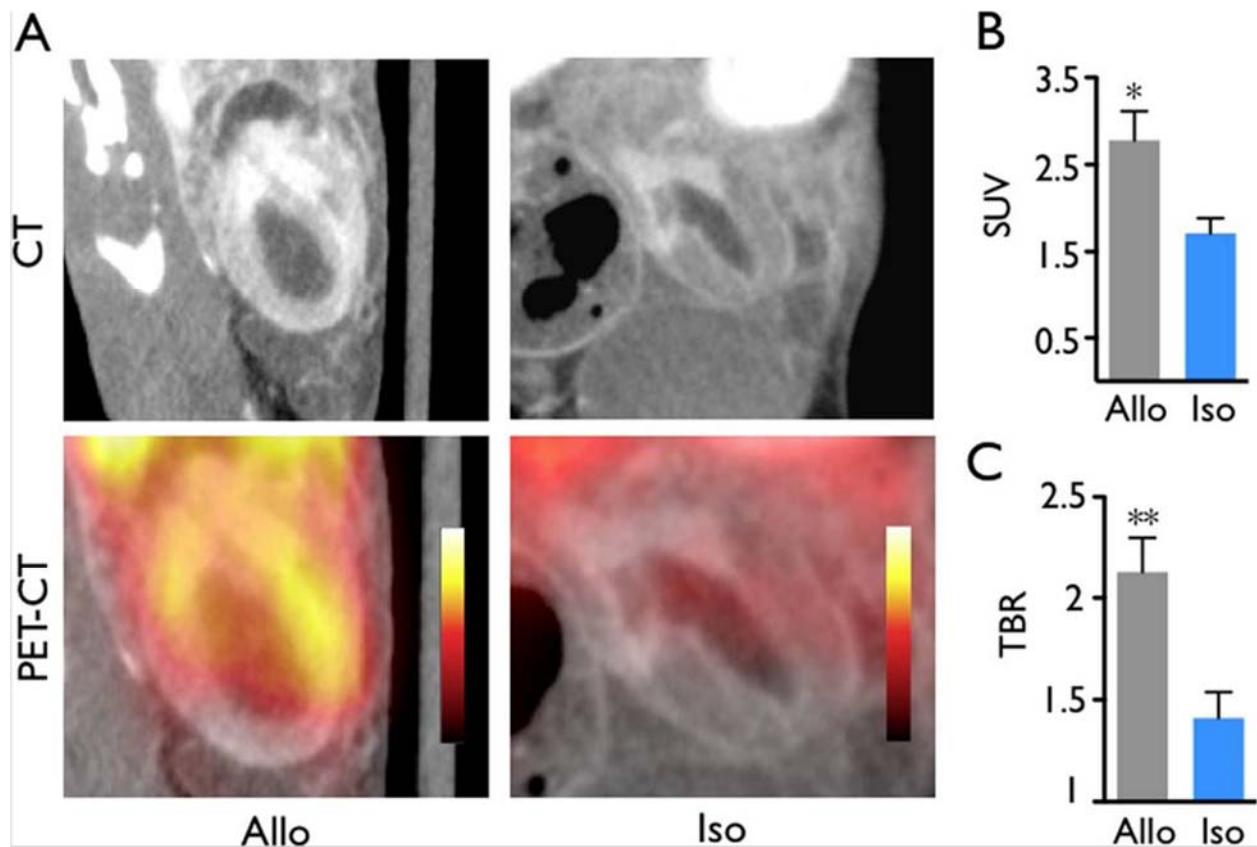


FIGURE 4. A. PET-CT images from reference 29 comparing inflammation in murine cardiac allo- and isografts on day 7 post-transplant. Animals were injected with ^{64}Cu -labeled dextran shell/iron oxide core nanoparticles 24 hours prior to imaging. The passively-targeted nanoparticles are effective reporters of graft inflammation, as they are known to undergo high levels of uptake by myeloid cells and negligible levels of uptake by other cardiac cells. **B & C.** Quantification of PET images. Allografts exhibited significantly greater standard uptake values (SUVs) and target:background ratios (TBRs) than isograft controls, demonstrating the potential utility of the dextran/iron oxide nanoparticles in assessment of graft rejection. Data are mean \pm SEM (* $P < 0.05$, ** $P < 0.01$). Reprinted from reference 29.

TABLE 1: Summary of select nanoparticle applications in nuclear cardiovascular imaging

Imaging target	Particle type	Mean diameter	Targeting strategy	Labeling agents	Imaging modalities	Reference
Ischemic myocardium	Polymeric micelles	7-20 nm	passive	¹¹¹ In	γ-camera	5
	Chitosan nanoparticles	100-150 nm	passive	^{99m} Tc	autoradiography	6
Ischemic brain	Liposomes	210 nm	passive	¹⁸ F	PET	7
Angiogenesis	Dendrimers	12 nm (pre-labeling)	RGD peptide (binds α _v β ₃)	⁷⁶ Br	PET-CT	9
	Comb-like polymeric nanoparticles	22 nm	C-type atrial natriuretic factor	⁶⁴ Cu	PET-CT	14
	Gold nanoparticles	22 nm	RGD peptide (binds α _v β ₃)	^{99m} Tc, gold	SPECT-CT	10
	Perfluorocarbon emulsion	270 nm	Non-peptide α _v β ₃ antagonist	^{99m} Tc, Gd ³⁺ , fluorophores	SPECT-CT/MR	11
	Single-walled carbon nanotubes	1-5 nm x 100-300 nm	RGD peptide (binds α _v β ₃)	⁶⁴ Cu, carbon nanotubes	PET, Raman spectroscopy (<i>ex vivo</i>)	12
	Polymer coated upconversion nanophosphors (UCNPs; NaGdF ₄ :Yb ³⁺ /Er ³⁺)	32 nm	RGD peptide (binds α _v β ₃)	¹²⁴ I, UCNP	PET-MR, upconversion luminescence (<i>ex vivo</i>)	13
Blood pool	Dendrimers	12 nm	passive	^{99m} Tc, 2,3,5-triiodobenzoic acid (TIBA)	SPECT-CT	15
	Cross-linked dextran shells/iron oxide cores	20 nm (base particle)	passive	¹⁸ F, iron oxide, fluorophores	PET-CT/MR, fluorescence (<i>ex vivo</i>)	16
	Core-shell star copolymers	25-70 nm	passive	⁶⁴ Cu	PET-CT	17
Atheromata	LDL	20 nm	Apolipoproteins (bind LDL receptor)	¹²³ I	γ-camera	19
	Reconstituted HDL particles with quantum dot (QD)/ iron oxide cores	8-12 nm	Apolipoproteins (bind HDL receptor)	⁵⁹ Fe, CdSe/CdS/ZnS QDs, iron oxide	MR, fluorescence, γ-counter (<i>ex vivo</i>)	22
Atheromata (intraplaque inflammation)	Dendrimers	n/a	LyP-1 peptide (binds macrophages)	⁶⁴ Cu, fluorophores	PET-CT, fluorescence (<i>ex vivo</i>)	24
	Comb-like polymer nanoparticles	15 nm	DAPTA (modified peptide, binds chemokine receptor-5)	⁶⁴ Cu	PET-CT	25
	Dextran nanoparticles	13 nm	passive	⁸⁹ Zr, fluorophores	PET-MR, autoradiography, fluorescence (<i>ex vivo</i>)	26
Cardiac allografts (graft inflammation)	Cross-linked dextran shells/iron oxide cores	20 nm	passive	⁶⁴ Cu, iron oxide, fluorophores	PET-CT, autoradiography, fluorescence (<i>ex vivo</i>)	29
Aortic aneurysms (mural inflammation)	Cross-linked dextran shells/iron oxide cores	20 nm (base particle)	passive	¹⁸ F, iron oxide, fluorophores	PET-CT, autoradiography, fluorescence (<i>ex vivo</i>)	30